

Formation of TiN grid on NiTi by laser gas nitriding for improving wear resistance in Hanks' solution

C.H. Ng, O.K. Chan, H.C. Man*

Department of Industrial and Systems Engineering, The Hong Kong Polytechnic

University, Hong Kong, China

*corresponding author: hc.man@polyu.edu.hk

Abstract

Laser gas nitriding (LGN) is a common surface modification method to enhance the wear resistance of Titanium (Ti) alloys, which are known to have poor tribological properties. In the present study, a titanium nitride (TiN) grid network was fabricated on the surface of nickel titanium (NiTi) by LGN. The laser processing parameters were selected so as to achieve nitriding without surface melting and hence to maintain a smooth surface finish. The characteristics of the grid-nitrided samples were investigated using scanning-electron microscopy (SEM), X-ray diffractometry (XRD), optical microscopy (OM), 2-D profilometry, contact angle measurements and nanoindentation. The wear resistance of the nitrided samples was evaluated using reciprocating wear test against ultra-high-molecular-weight polyethylene (UHMWPE) in Hanks' solution. The results indicate that the wear rates of the grid-nitrided samples

and the UHMWPE counter-body in the wear pair are both significantly reduced. The decrease in wear rates can be attributed to the combination of a hard TiN grid and a soft NiTi substrate. In Hanks' solution the higher hydrophilicity of the nitrided samples also contributes to the better performance in wear test against hydrophobic UHMWPE.

Keywords: Laser; Nitriding; Surface patterning; Titanium alloys; Wear

1. Introduction

Titanium (Ti) alloys possess many attractive properties, including high specific strength and modulus, good biocompatibility and excellent corrosion resistance [1-5]. Among the Ti alloys, nickel-titanium (NiTi) alloy is particularly attractive by virtue of its well-known shape memory effect and super-elasticity, which make it a popular material in various biomedical applications, such as vascular stents, staples and bone plates for fracture fixation [6-8]. Though NiTi is not currently used as the major component in total hip or knee replacement implants, it has been recommended as a highly potential material for such orthopedic applications in a recent article [9] which evaluated 10 metallic materials in current use (such as Ti6Al4V and CoCrMo) and potential materials (such as NiTi). The evaluation was based on holistic consideration of 7 properties: density, tensile strength, modulus of elasticity, elongation, corrosion

resistance, wear resistance, and osseointegration. Nevertheless, similar to other Ti alloys, there is a concern of the relatively poor wear properties of NiTi alloys in potential orthopedic applications where they are in contact with polymeric counterparts [10-12]. The formation of a wear resistant layer such as TiN on the surface of NiTi and Ti alloys is a promising method to enhance their wear properties due to its low chemical reactivity, high hardness and low friction coefficient [13-14]. There are various methods of forming TiN layer or film on Ti alloys, each with its advantages and shortcomings. Chemical vapour deposition (CVD) and physical vapour deposition (PVD) are popular methods for surface nitriding. Nevertheless, these methods are suitable for forming a nitride film on the whole sample surface [15-16]. In the present investigation we propose a new surface modification technique in which a network of nitride grids is fabricated on the sample surface instead of forming a continuous nitride layer. To achieve such an aim laser technique is particularly suitable because of the ease of control of the nitrified location. Using laser technique to form nitride grids may be regarded as a variant of laser surface texturing, which is becoming popular for improving wear resistance [17]. Moreover, in most of the conventional nitriding methods the substrate temperature reaches the range 400-1000 °C, which has an undesirable effect on the mechanical properties of Ti alloys in general and NiTi in particular, because of its special thermomechanical

characteristics. On the other hand, the substrate temperature only rises slightly in laser gas nitriding (LGN). LGN on Ti alloys was attempted by Katayama et al. in 1983 and a wide variety of research studies have continued since then [18-20]. However, LGN generally involves melting of the titanium surface and it results in a roughened surface after treatment, and the roughened surface would not be desirable in tribological applications. To prevent surface roughening after LGN, we aim at laser gas nitriding of NiTi without surface melting by selecting suitable laser processing parameters in the present study, so that TiN is formed via solid-state diffusion. To improve the tribological behavior of the substrate via nitriding or other types of surface modification, it is common to treat the whole sample surface. It is interesting to study nitriding on a sample to form a nitride grid instead of a continuous layer on the surface, which is a form of laser texturing or patterning, and to study its effect on the wear performance in the wear pair.

2. Experimental Methods

2.1 Materials

NiTi plates (Ti–55.91 wt% Ni) was used in this study and samples of dimensions 40 mm x 30 mm x 5 mm were spark cut from NiTi plates. Before LGN, the surface of the samples was polished sequentially with a series of SiC papers down to 1200 grits

to remove oxide scale, followed by polishing with 1 μ m diamond paste. Subsequently the samples were cleaned and degreased ultrasonically in methanol bath for 10 min, rinsed in distilled water, and dried thoroughly in cold air stream prior to LGN.

2.2 Laser Gas Nitriding (LGN)

The LGN process was performed using a 100 W CW fiber laser (SP-100C-0013, SPI and A&P Co., Ltd) with a wavelength of 1091 nm. The samples were positioned in a chamber which was continuously purged with pure nitrogen gas at a rate of 40 L/min to create a nitrogen atmosphere during LGN. The flow rate of nitrogen gas was controlled by flow meters from two nozzles, one being the axial nozzle and the other, for the chamber. The gas flow rate of axial nozzle was set at appropriate values so as to minimize plasma formation and in-drag of oxygen. The laser power was set at 90 W for the LGN. In order to select parameters for nitriding without melting, the laser spot diameter was varied from 0.5 mm to 2.2 mm, and the laser scanning speed was varied from 60 mm/min to 1500 mm/min. After selecting the suitable parameters for nitriding, nitride tracks were fabricated on the sample surface to form a network of grids having different fractions of nitride coverage, as shown in Figure 1.

2.3 Characterization

Optical microscopy (OM, Leica DM4000M) was used for preliminary observation of the surface morphology of the laser-treated samples. Cross-section of laser tracks on the samples was studied using scanning-electron microscope (SEM, JEOL Model JSM-6490). The phases present in the nitrided and untreated NiTi samples were identified using X-ray diffraction (XRD, Rigaku SmartLab) at 40 kV and 40 mA using $\text{CuK}\alpha$ radiation for the 2θ ranging from 30° to 80° .

The surface roughness R_a of laser-nitrided and untreated samples was measured using a surface profilometer (Talysurf Series 2). To study the wetting behavior of the samples, measurement of contact angle of Hanks' solution (a simulated body fluid with composition shown in Table 1) on the samples was performed [15]. The samples were cleaned with ethanol bath ultrasonically for 5 min and then dried thoroughly in cool air before measurement. A microsyringe was used to deliver droplets of Hanks' solution onto the sample surface (5 μl / droplet). By using an optical meter equipped with CCD video camera, the images were captured and studied using an image processing software (contact angle goniometer Sindatek Model 100SB).

As the nitride layer was only around 1 to 2 μm in thickness, nanoindentation tests employing a diamond Berkovich indenter were performed on untreated and nitrided NiTi (Hysitron nanomechanical test instrument, HLS1 module). Loading and unloading curves were acquired and the hardness H_N and reduced Young's modulus

Er were determined from the curves. 5 duplicates of each type of samples were used for calculating the mean values and errors.

2.4 Wear Test

The acetabular cup and the tibial plateau in human joint replacement are usually made of ultra-high-molecular-weight polyethylene (UHMWPE) [21], and titanium or titanium alloys are recommended materials for the femoral components [22]. Recent studies on the tribological behavior of titanium alloys against UHMWPE have been reported [23,24], which indicated that the long-term performance of UHMWPE in the wear pair is a major factor for the life of total hip prostheses [25]. Consequently, reciprocating wear test was employed to evaluate the wear properties of grid-nitrided and untreated NiTi samples against UHMWPE. Linearly reciprocating pin-on-plate sliding test was performed (TE99 Universal Wear Machine, Phoenix Tribology). A flat-ended UHMWPE pin with 8 mm diameter was fixed in the sliding carriage clamped and pressed endwise against the counterface plate, which was the NiTi sample. The diameter of the UHMWPE pin was chosen so that it was always in contact with both the nitrided and untreated surface. The reciprocating pin-on-plate sliding test was carried out at a normal load of 96 N, a frequency of 2 Hz, and of stroke length 30 mm, for test duration of 172,800 cycles (about 10 km of sliding

distance) in Hanks' solution, which is a simulated body fluid. The wear resistance was evaluated using the wear factor ($= \text{wear volume (mm}^3\text{)}/\text{load (N)} \times \text{distance travelled (m)}$) for comparison of wear rates of different samples. For each type of samples, 5 duplicates were tested and the mean value together with the errors was calculated.

3. Results and Discussion

3.1 Parameters selection

When the surface of the NiTi substrate is irradiated with a laser beam, part of the laser energy is absorbed by the substrate and the temperature of the surface rises. In a nitrogen atmosphere, TiN is formed due to the great affinity of Ti for nitrogen. Depending on the amount of laser power density absorbed, the surface may or may not melt. Thus in order to achieve nitriding without surface melting, the laser processing parameters, which include the laser power (P), laser spot diameter (d) and laser scanning speed (v), have to be carefully selected. In the present investigation, the laser power was fixed and the spot diameter and scanning speed were varied to efficiently fabricate TiN tracks without surface melting. To achieve this goal, the feasible processing parameters identified are laser power $P = 90$ W, scanning speed $v = 60$ mm/min and spot diameter $d = 2.2$ mm, with nitrogen flow rate at 40 L/min, the laser fluence being 40.9 J/mm^2 under this set of parameters. Laser nitrided tracks with

different separations were then fabricated on the sample surface to form networks of grids with different areas of nitride coverage (Figure 1).

3.2 Characteristics of nitride layer

After LGN the sample surface shows a golden color, which suggests the formation of TiN. The cross-sectional SEM micrograph of a typical non-melted nitride track is shown in Figure 2. A uniform layer of thickness of around 1.76 μm could be clearly observed. TiN dendrites and heat-affected zones are absent due to the low laser fluence in the present case of solid-state nitriding, which aims at producing TiN coating without changing the surface roughness of the NiTi samples.

The X-ray diffraction patterns for the untreated and laser treated tracks are shown in Figure 3. TiN peaks are present in the patterns for the laser treated tracks, evidencing the formation of a thin TiN layer on the NiTi. These peaks correspond to cubic titanium nitride (TiN) at (200) and (310). On the untreated NiTi sample only the austenite phase (also known as the B-2 phase, or the FCC phase) is present (Figure 3).

The formation of the nitrated layer on a titanium alloy is more complicated than on pure Ti. Nitrogen (N) absorbed at the surface under laser irradiation diffuses inward into NiTi at elevated temperatures. Rapid diffusion of N into the surface of NiTi during laser treatment will first form an interstitial solution in NiTi. Upon

saturation of this interstitial solution, TiN will eventually be formed due to the great affinity of Ti for N [26]. When TiN is formed on the surface NiTi by consuming Ti from the substrate, a Ni-rich phase will be formed somewhere, due to conservation of matter. According to a recent study on nitriding of Ti-6Al-4V by Morgiel and Wierzchon [27], Al was “pushed out” to beneath the TiN layer. In fact, XPS study of the surface layer of laser gas nitrided NiTi in one of our previous publications [28] clearly shows that Ni was absent in the nitrided layer of NiTi, similar to the “pushing out” of Al in [27]. This “pushing out” of Ni to beneath the surface layer was also reported in thermal oxidation of NiTi by Firstov et al. [29].

The results of these studies indicate depletion of Ni in the surface layer after nitriding or oxidation of NiTi. In agreement with these results, a number of studies [28,30] also reported significantly reduced Ni ion release rate for NiTi nitrided by different processes, including laser gas nitriding by our group [28].

The topography and roughness of the surface layer after LGN depend strongly on the laser processing parameters, i.e., the laser fluence. To investigate changes in surface roughness, 2-D surface profiles were acquired using a surface profilometer (Talysurf series 2). Typical surface profiles of untreated NiTi sample, nitrided NiTi samples with and without surface melting are shown in Figure 4. The surface roughness R_a was significantly increased from 0.0074 μm (untreated) to 0.0226 μm

(surface melting). The large difference in the surface roughness is attributed to surface melting and subsequent solidification during conventional LGN with high heat input and slow cooling rate [31]. Nitrogen atoms react with the melt pool to form a thick TiN layer, which has a relatively large roughness. On the contrary, the surface roughness of the substrate which was nitrided without melting is almost the same compared with the untreated sample. This result is in agreement with the findings of a pervious study [32]. Post surface treatment like polishing is thus not needed and this is an important advantage of solid-state nitriding as compared with conventional nitriding involving melting.

Nanoindentation test is commonly used for determination of the mechanical properties of thin film due to its capability of continuously applying a small load. The resulting indentation depth is small so that substrate effect can be significantly reduced [33]. Moreover, the instrumented loading and unloading allows continuous capturing of the load-displacement curves, and from these curves important mechanical properties like the reduced Young's modulus E_r and the hardness H_N can be obtained [34]. Although the substrate effect can be greatly reduced using a very small load, surface roughness effect sets a restriction on the load, which cannot be too small, otherwise the nanoindentation curves would be become very noisy. Thus an appropriate loading force and the corresponding indentation depth should be selected.

In the present study the load selected was 50000 μN , and the corresponding indentation depth for the nitride layer was around 450 nm, which is about 25 % of the nitride layer thickness. This loading is an optimal selection as it resulted in a smooth load-displacement curve while the indentation depth is acceptably small. Figure 5 shows typical nanoindentation curves for the NiTi substrate and the TiN coating. The hardness H_N and reduced Young's modulus E_r were extracted from the load-displacement curves. The nitride layer coating exhibits much higher values in hardness H_N (17.92 ± 3.69 GPa) and reduced Young's modulus E_r (131.65 ± 8.04 GPa) than the NiTi substrate (H_N of 4.44 ± 0.55 GPa and E_r of 66.28 ± 2.54 GPa). The hardness and reduced Young's modulus of the nitride layer are about 4 times and 2 times of untreated NiTi, respectively. The ratio of hardness to reduced Young modulus has been proposed as an important factor in determining wear resistance [35]. By comparing the nitride layer and the NiTi substrate, the H_N/E_r ratio of NiTi substrate (0.066) is about half that of the nitride layer (0.136). The higher value of H_N/E_r ratio of the nitride layer is in agreement with the results of Cheng et al. [36].

Figure 6 shows the wettability results for the untreated NiTi and nitrided NiTi in Hanks' solution. As shown in Figure 6, the liquid droplet on the surface of nitrided NiTi has a contact angle of $62.34 \pm 2.74^\circ$, which is smaller than that on untreated NiTi ($67.06 \pm 2.26^\circ$). This indicates that nitrided NiTi is more hydrophilic. In the paper by

Borruto et al. [37], it was pointed out that the wetting behaviors of the contacting surfaces in a tribological pair would significantly affect the wear behavior of the pair. It was concluded there that a hydrophilic-hydrophobic coupling enhances the efficiency of lubrication due to the presence of pressed water film between the pair. This film results in low wear rate and low friction coefficient in the tribological system. As UHMWPE is hydrophobic, the better hydrophilicity of the nitrided NiTi in Hanks' solution would enhance lubrication and reduce friction and wear between nitrided NiTi and UHMWPE.

3.3 Wear behavior of untreated and grid-nitrided NiTi

To study the effect of grid-nitriding on wear performance, reciprocating wear tests between UHMWPE and NiTi samples were performed in Hanks' solution. The wear resistance is evaluated by using the wear factor, which is the wear volume per unit normal load per unit sliding distance, and is a parameter commonly used in the biomaterials community [38]. A higher wear factor indicates more serious wear damage and hence lower wear resistance. Figure 7 shows the wear factor of UHMWPE, untreated and various grid-nitrided NiTi samples after 172,800 cycles in the test, based on the results of 5 duplicate pairs. The small error bars in Figure 7 indicate that the wear test results are acceptably reliable.

The wear test results demonstrate that grid-nitrided NiTi exhibits better wear performance than that of untreated NiTi in the wear pair. It is clearly seen that the wear rates for both NiTi and UHMWPE were significantly reduced in the nitrided-NiTi/UHMWPE pair.

The friction coefficient between UHMWPE and the NiTi counterparts in the reciprocating wear tests are summarized in Table 2. Obviously, the friction coefficient for grid-nitrided NiTi is lower than that for untreated NiTi.

The wear factor ratio of the nitrided-NiTi/UHMWPE pair compared with bare-NiTi/UHMWPE pair for different percentages of TiN area coverage is shown in Figure 8. It indicates that as the TiN area coverage increases, the wear volume losses of TiN and UHMWPE both decrease. However, when the TiN area coverage increases from 35% to 55%, the wear factor ratio of TiN and UHMWPE are nearly the same. Going beyond 55% TiN area coverage, the wear factor ratio drops again in both of TiN and UHMWPE. TiN is much higher in hardness than NiTi and has a higher wear resistance. Thus increasing the area coverage by TiN favors enhancing wear performance. On the other hand, the grooves in the network provide room for wear debris formed, which would otherwise stay on the surface and become detrimental to friction and wear as a third body.

Stereoscopic optical morphology of the surface of UHMWPE pin before and after the wear test is shown in Figure 9. It can be observed that the machined pattern on the UHMWPE pin against untreated NiTi has totally disappeared while that on the pin against grid-nitrided NiTi is still visible, indicating a lower wear rate of the UHMWPE pin in the latter case. Figure 10 shows the appearance of NiTi after the wear test. UHMWPE transferred layers were formed on the untreated NiTi plate surface. It was associated with a relatively high coefficient of friction of untreated NiTi sample. On the other hand, there is no UHMWPE transferred layer formed on the grid-nitrided NiTi. The above experimental results indicate that the grid-nitrided NiTi/UHMWPE pair exhibits much better wear performance than that consisting of untreated NiTi and UHMWPE.

4. Conclusions

Laser gas nitriding (LGN) on NiTi has been endeavored with an aim of obtaining the nitrided surface without melting. Friction and wear performance of treated and untreated NiTi in Hanks' solution in reciprocating test have been compared. The following concluding remarks could be made.

1. With the laser power and nitrogen gas flow rate fixed at 90 W and 40 L/min, the optimal laser scanning speed and laser spot diameter are respectively 60 mm/min

and 2.2 mm for achieving solid-state nitriding. The thickness of nitride layer is about 1.76 μm .

2. Nitriding of NiTi improves the wear performance of the NiTi/UHMWPE wear pair in Hanks' solution, as evidenced by the significant reduction in wear rates for both contact materials in the pair. This could be attributed to a higher H_N/Er ratio of the nitride layer, and to a lower coefficient of friction. In addition, the wear factors decrease with increasing area of nitride coverage.
3. Nitriding of NiTi increases its hydrophilicity in Hanks' solution. A hydrophilic (nitrided NiTi)/hydrophobic (UHMWPE) friction couple promotes the efficiency of lubrication and further reduces the wear rate.

The results of the present investigation indicate that laser grid-nitriding of NiTi via solid-state diffusion is an effective process for improving the tribological performance of the NiTi/UHMWPE wear pair in Hanks' solution.

Acknowledgement

The authors' work in this paper was supported by a research grant (Project No. PolyU 524210E) from the Research Grants Council of the Hong Kong Special Administrative Region, China.

References

- [1] Polmear IJ. Light alloys. The metallurgy of the light metals. Edward Arnold
1989;2:265-268
- [2] Castleman LS, Motzkin SM, Alicandri FP. Biocompatibility of nitinol alloy as an
implant material. J Biomed Mater Res 1976;10:695-731
- [3] Prince MR, Salzman EW, Schoen FJ, Palestrant AM, Simon M. Local
intravascular effects of the nitinol wire blood clot filter. Invest Radiol
1988;23:294-300
- [4] Kasano F, Morimitsu T. Utilization of nickel-titanium shape memory alloy for
stapes prosthesis. Auris Nasus Larynx 1997;24:137-142
- [5] Ryhanen J, Kallioinen M, Serlo W, Peramaki P, Junila J, Sandvik P, et al. Bone
healing and mineralization, implant corrosion, and trace metals after nickel-titanium
shape memory metal intramedullary fixation. J Biomed Mater Res 1999;47:472-480
- [6] Humbeeck JV. Preface to the viewpoint set on: shape memory alloys. Scr Mater
2004;50:179-180
- [7] Kennedy JB. In: Funakubo (Ed.), shape memory alloys. New York: Gordon and
Breach Science Publishers; 1987. p. 226.
- [8] Duerig T, Pelton A, Stochel D. An overview of nitinol medical applications. Mater
Sci Eng A 1999;273-275:149-160.

- [9] Bahraminasab M and Jahan A. Material selection for femoral component of total knee replacement using comprehensive VIKOR. *Materials and Design* 2011;32: 4471-4477.
- [10] Matsumoto K, Tajima N, Kuwahara S. Correction of scoliosis with shape-memory alloy. *Nippon Seikeigeka Gakkai Zasshi* 1993;67:267-274
- [11] Ryhanen J, Niemi E, Serio W, Niemela E, Sandvik P, Pernu H, et al. Biocompatibility of nickel-titanium metal and its corrosion behavior in human cell cultures. *J Biomed Mater Res* 1997;35:451-457
- [12] Rocher P, El Medawar L, Hornez J-C, Traisnel M, Breme J, Hildebrand HF. Biocorrosion and cytocompatibility assessment of NiTi shape memory alloys. *Scripta Mater* 2004;50:255-260
- [13] Kenneth GB. Tribological properties of titanium alloys. *Wear* 1991;151:203-217
- [14] Deng JX, Liu AH. Dry sliding wear behavior of PVD TiN, Ti55Al45N, and Ti35Al65N coatings at temperatures up to 600 °C. *Int J Refractory Metals Hard Mater* 2013;41:241-249
- [15] Budziak D, Martendal E, Carasek E. New poly(ethylene glycol) solid-phase microextraction fiber employing zirconium oxide electrolytically deposited onto a NiTi alloy as substrate for sol–gel reactions. *J Chromatogr A* 2008;1198-1199:54-58
- [16] Milosev Y, Navinsek B. A corrosion study of TiN (physical vapour deposition)

hard coatings deposited on various substrates. *Surf Coat Technol* 1994;63:173-180

[17] Perez MG, Harlan NR, Zapirain F, Zubiri F. Laser nitriding of an intermetallic

TiAl alloy with a diode laser. *Surf Coat Technol* 2006;200:5152-5159

[18] Katayama S, Matsunawa A, Morimoto A. In: A. Metzbower (Ed.), *Proceeding of*

Materials processing Symposium, vol. 38, Laser institute of America, Washington DC:

Naval Research Dept; 1983, p. 127.

[19] Abbound JH, Fidel AF, Benyounis KY. Surface nitriding of Ti-6Al-4V alloy with

a high power CO₂ laser. *Opt Laser Technol* 2008;40:405-414

[20] Lima MSF, Folio F, Mischler S. Microstructure and surface properties of

laser-remelted titanium nitride coatings on titanium. *Surf Coat Technol*

2005;199:83-91

[21] Besong AA, Tipper JL, Ingham E, Stone MH, Wroblewski BM, Fisher J.

Quantitative comparison of wear debris from UHMWPE that has and has not been

sterilised by gamma irradiation. *J Bone Joint Surg Br* 1998;80:340-344

[22] Semlitsch M. Titanium alloys for hip joint replacements. *Clin Mater* 1987;2:1-13

[23] Schmidt H, Schminke A, Ruck DM. Tribological behavior of ion-implanted

Ti6Al4V sliding against polymers. *Wear* 1997;209:49-56

- [24] Suhendra N, Stachowiak GW. Computational model of asperity contact for the prediction of UHMWPE mechanical and wear behaviour in total hip joint replacements. *Tribol Lett* 2007;25:9-22
- [25] Dumbleton JH, Manley MT, Edidin AA. A literature review of the association between wear rate and osteolysis in total hip arthroplasty. *J Anthroplasty* 2002;17:649-661
- [26] Malinov S, Zhecheva A, Sha W. Proceedings of the 1st International Surface Engineering Congress and the 13th IFHTSE Congress. ASM International. Materials Park, OH, 2003, p. 344.
- [27] Morgiel J and Wierzchon T. New estimate of phase sequence in diffusive layer formed on plasma nitrided Ti-6Al-4V alloy. *Surf. Coat. Technol.* 2014;259:473-482.
- [28] Man HC, Cui ZD, Yue TM. Surface characteristics and corrosion behavior of laser surface nitrided NiTi shape memory alloy for biomedical applications. *J. Laser App.* 2002;14:242-247.
- [29] Firstov GS, Vitchev RG, Kumar H, Blanpain B, Van Humbeeck J. Surface oxidation of NiTi shape memory alloy. *Biomaterials* 2002;23:4863-4871.
- [30] Starosvetsky D, Gotman I. TiN coating improves the corrosion behavior of superelastic NiTi surgical alloy. *Surf. Coat. Technol.* 2001;148:268-276.
- [31] Santos EC, Morita M, Shiomi M, Osakada K, Takahashi M. Laser gas nitriding

of pure titanium using CW and pulsed Nd:YAG lasers. *Surf Coat Technol* 2006;201:1635-1642

[32] Man HC, Bai M, Cheng FT. Laser diffusion nitriding of Ti-6Al-4V for improving hardness and wear resistance. *App Surf Sci* 2011;258:436-441

[33] Tsui TY, Vlassak J, Nix WD. Indentation plastic displacement field: Part II. The case of hard films on soft substrates. *J Mater Res.* 1999;14:2196-2203

[34] Oliver WC, Pharr GM. An improved technique for determining hardness and elastic modulus using load and displacement sensing indentation experiments. *J Mater Res* 1992;7:1564-1583

[35] Ni WY, Cheng YT, Lukitsch MJ, Weiner AM, Lev LC, Grummon DS. Effects of the ratio of hardness to Young's modulus on the friction and wear behavior of bilayer coatings. *Appl Phys Lett* 2004;85:4028-4030

[36] Cheng Y, Zheng YF. Formation of TiN films on biomedical NiTi shape memory alloy by PIIID. *Mater Sci Eng A* 2006;434:99-104

[37] Borruto A, Marrelli L, Palma F. The difference of material wettability as critical factor in the choice of a tribological prosthetic coupling without debris release. *Tribol Lett* 2005;20:1-10.

[38] *Handbook of Biomaterials Evaluation: Scientific, Technical, and Clinical Testing of Implant Materials*”, 2nd ed., edited by A.F. von Recum, Taylor & Francis, 1999.

Figure Captions

Figure 1. Grid-nitrided NiTi with different fractions of nitride coverage.

Figure 2. SEM cross-sectional view of a non-melted nitride track.

Figure 3. XRD patterns of the untreated substrate and laser treated tracks.

Figure 4. Surface profile of the (a) untreated sample, (b) melted track and (c) non-melted track.

Figure 5. Typical nanoindentation curves of (a) untreated NiTi and (b) nitride track.

Figure 6. Images of contact angles of Hanks' solution droplet resting on the surface of treated and untreated NiTi.

Figure 7. Wear factor of grid-nitrided NiTi against UHMWPE in Hanks' solution.

Figure 8. Wear factor ratio of the nitrided-NiTi/UHMWPE pair compared with that of bare-NiTi/UHMWPE pair for different percentages of TiN area coverage.

Figure 9. Optical images of the surface of UHMWPE pin against untreated NiTi and grid-nitrided NiTi (35%).

Figure 10. Optical images of the surface of untreated NiTi and nitrided NiTi.

Table 1. Composition of Hanks' solution.

Table 2. Coefficient of friction of UHMWPE in reciprocating sliding test

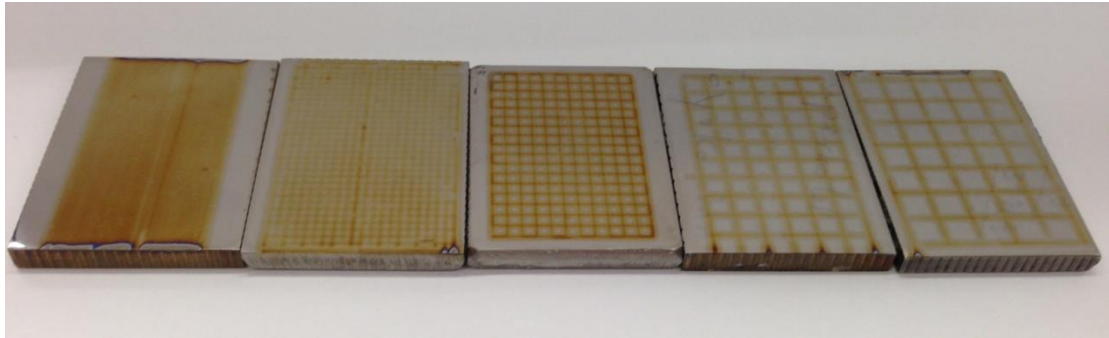


Figure 1. Grid-nitrided NiTi with different fractions of nitride coverage.

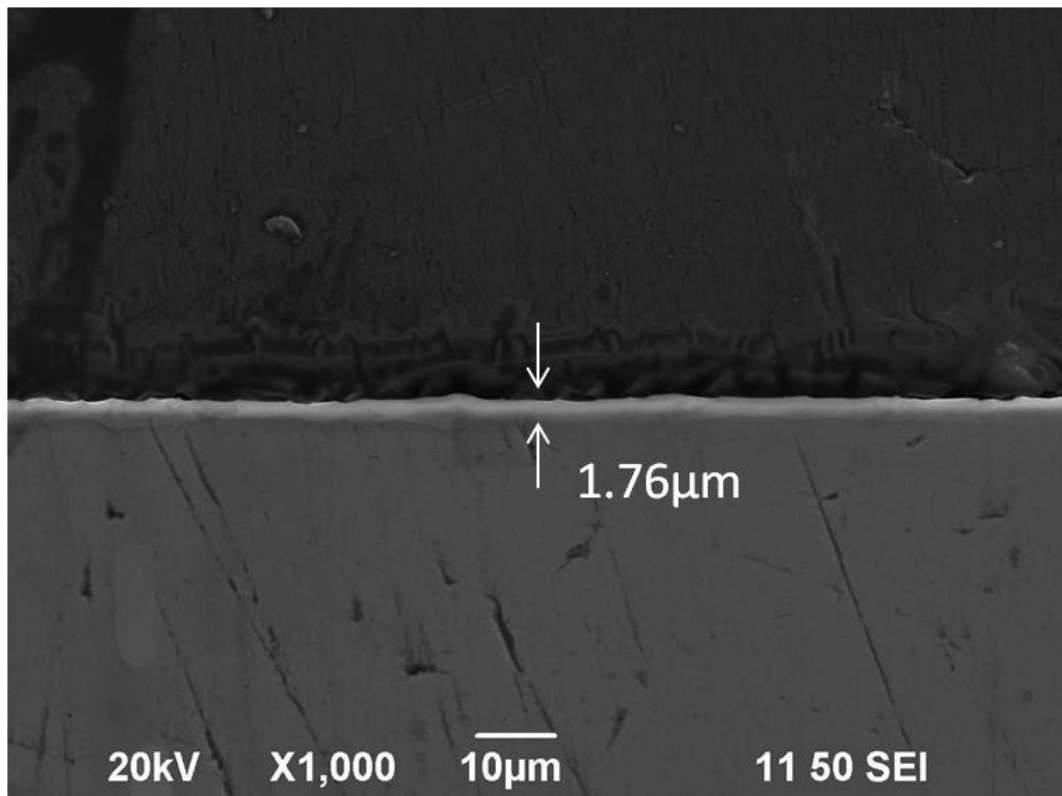


Figure 2. SEM cross-sectional view of a non-melted nitride track.

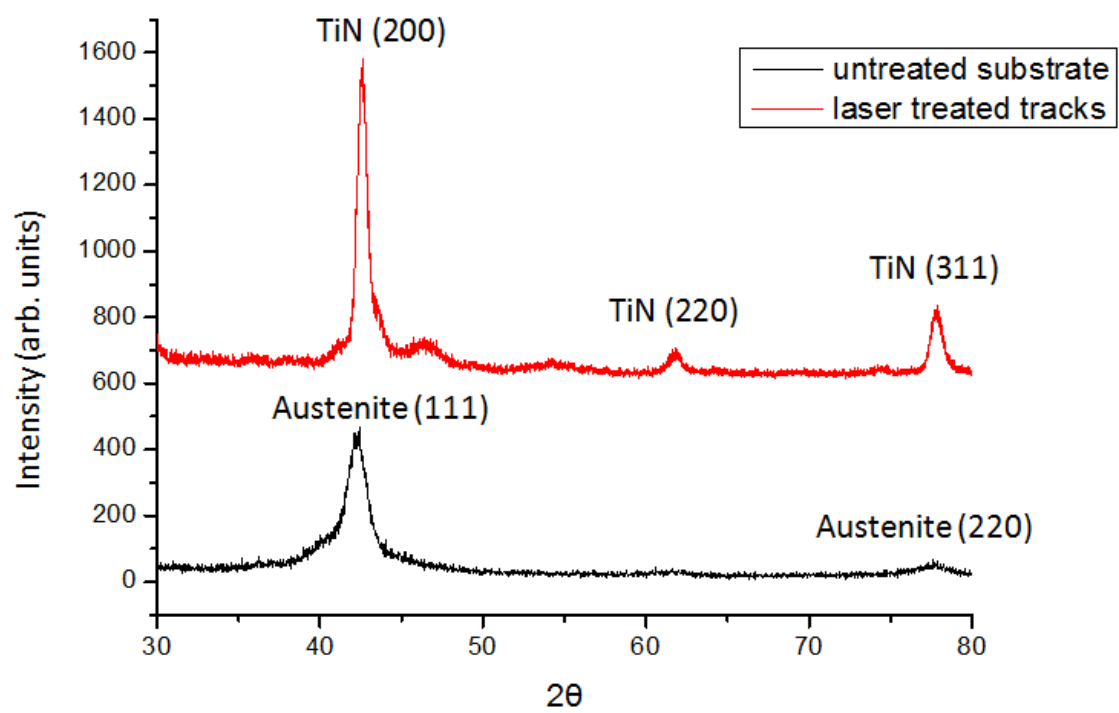
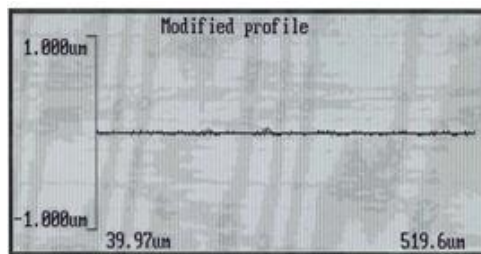
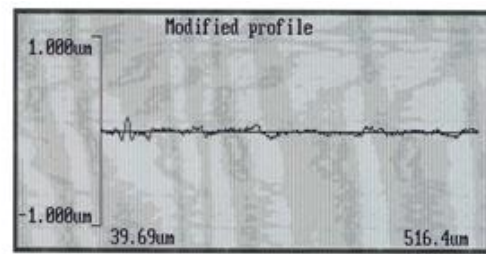


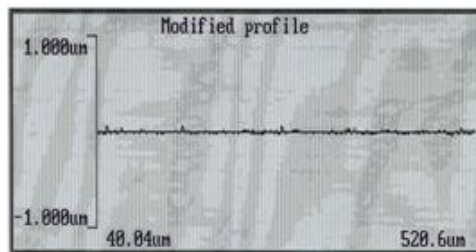
Figure 3. XRD patterns of the untreated substrate and laser treated tracks.



(a) Untreated
 $R_a = 0.0074 \mu\text{m}$

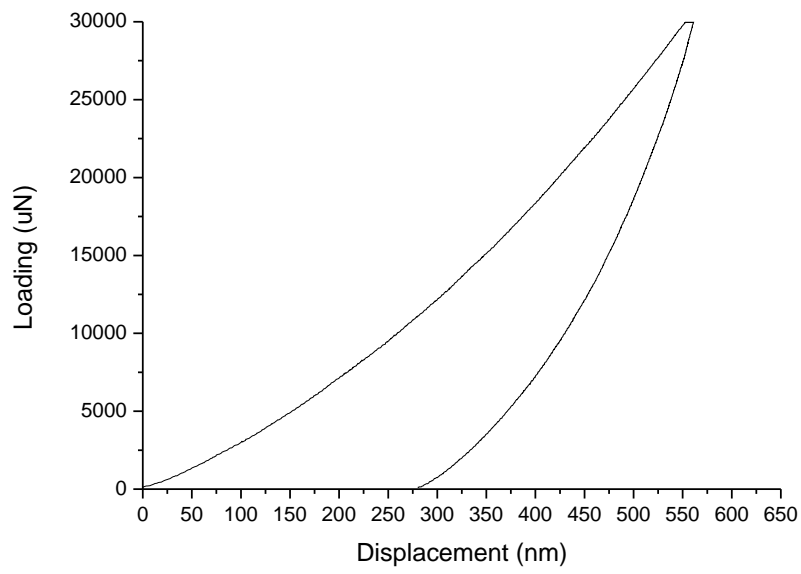


(b) Melted Track
 $R_a = 0.0226 \mu\text{m}$

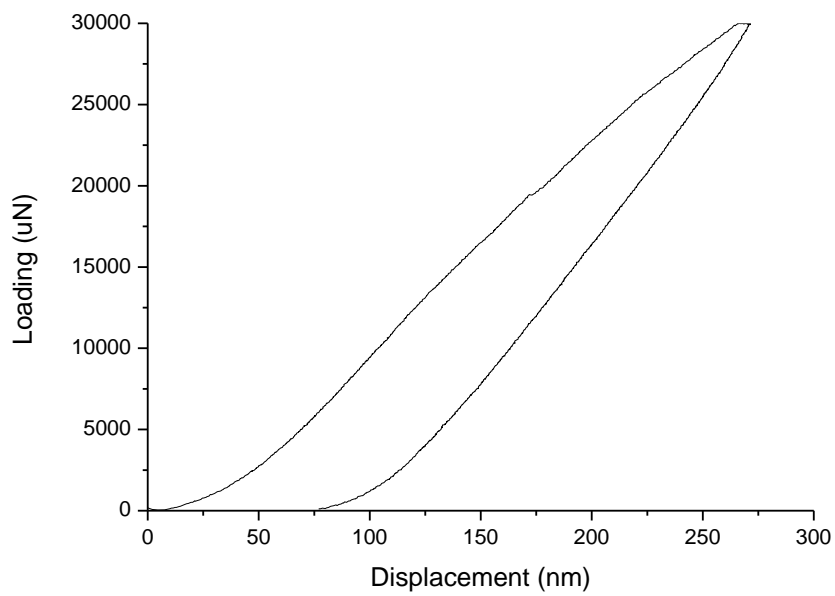


(c) Non-melted Track
 $R_a = 0.0092 \mu\text{m}$

Figure 4. Surface profile of the (a) untreated sample, (b) melted track and (c) non-melted track.



(a)



(b)

Figure 5. Typical nanoindentation curves of (a) untreated NiTi and (b) nitride track.



Untreated NiTi	Nitrided NiTi
	
$67.06 \pm 2.26^\circ$	$62.34 \pm 2.74^\circ$

Figure 6. Images of contact angles of Hanks' solution droplet resting on the surface of
treated and untreated NiTi

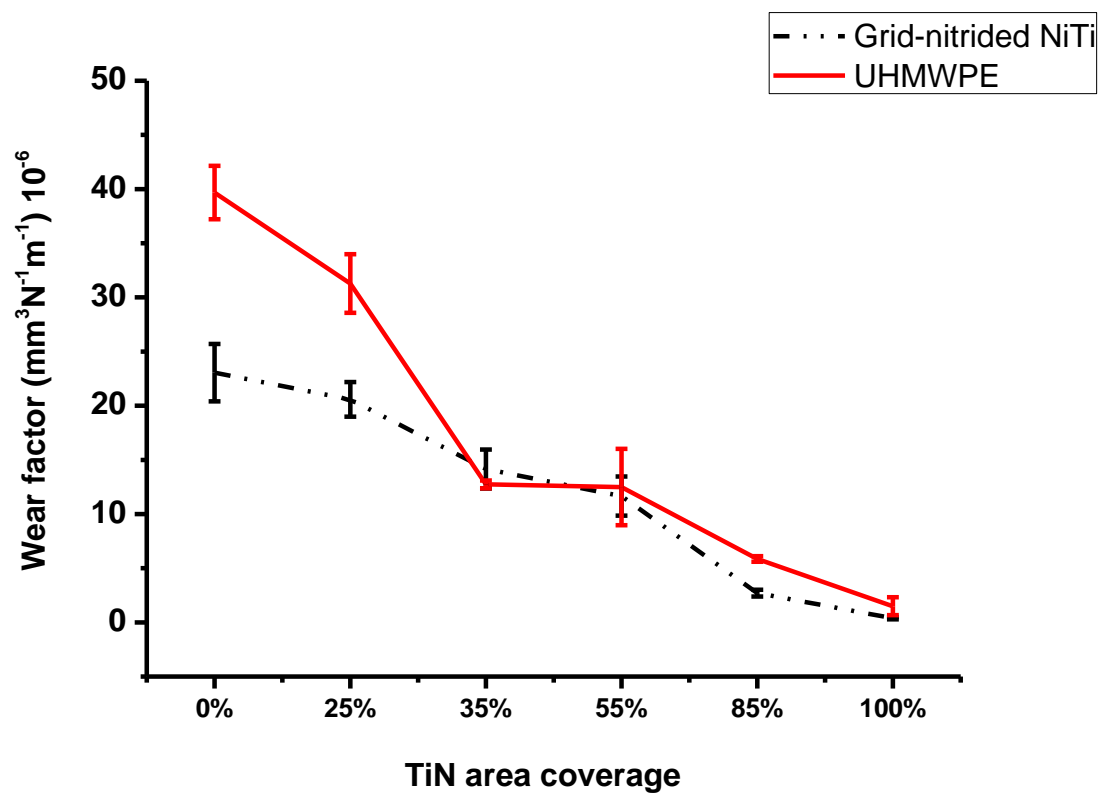


Figure 7. Wear factor of grid-nitrided NiTi against UHMWPE in Hanks' solution.

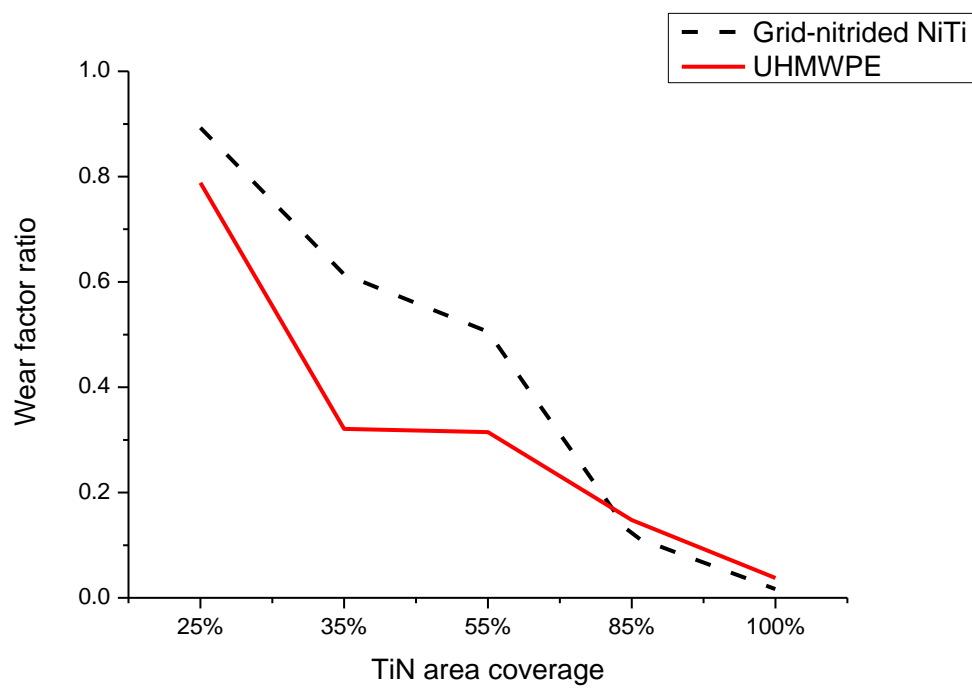


Figure 8. Wear factor ratio of the nitrided-NiTi/UHMWPE pair compared with that of bare-NiTi/UHMWPE pair for different percentages of TiN area coverage.





	Before	After
Untreated NiTi		
Grid-nitrided NiTi (35%)		

Figure 9. Optical images of the surface of UHMWPE pin against untreated NiTi and grid-nitrided NiTi (35%).

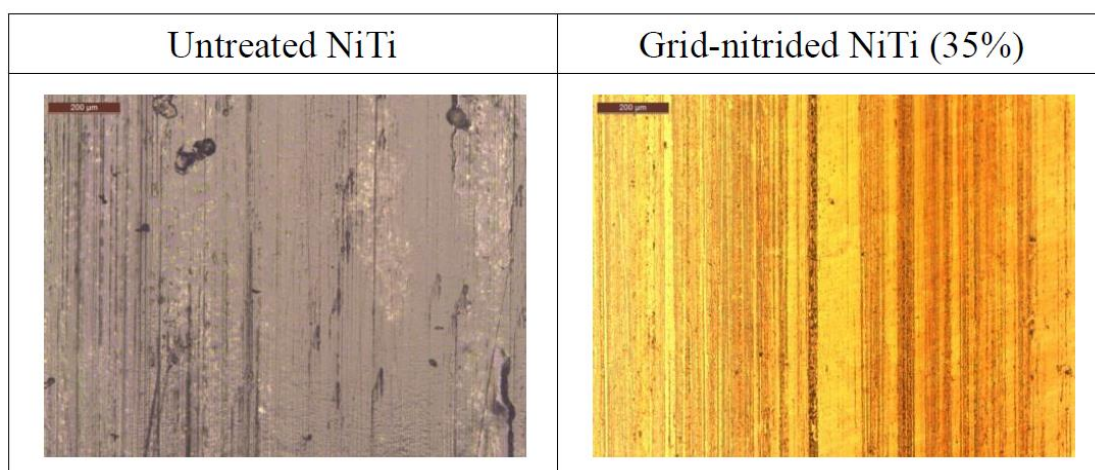


Figure 10. Optical images of the surface of untreated NiTi and nitrided NiTi.

Component	Concentration (g/l)
Sodium Chloride	8
Potassium Chloride	0.4
Potassium Phosphate, monobasic	0.06
Glucose	1
Phenol Red, Na salt	0.01
Sodium Phosphate, dibasic	0.048
Sodium Bicarbonate	0.35

Table 1. Composition of Hanks' solution.

	Friction coefficient	
	Initial stage	Stable stage
Untreated NiTi (0%)	0.02 ± 0.02	0.14 ± 0.02
Grid-nitrided (25%)	0.02 ± 0.02	0.07 ± 0.02
Grid-nitrided (35%)	0.02 ± 0.02	0.04 ± 0.02
Grid-nitrided (55%)	0.02 ± 0.01	0.04 ± 0.02
Grid-nitrided (85%)	0.03 ± 0.01	0.04 ± 0.01
Grid-nitrided (100%)	0.03 ± 0.01	0.04 ± 0.01

Table 2. Coefficient of friction of UHMWPE in reciprocating sliding test.